Eur. Phys. J. C (2016) 76:706
DOI 10.1140/epjc/s10052-016-4561-3

THE EUROPEAN PHYSICAL JOURNAL C

Regular Article - Theoretical Physics

The new interaction suggested by the anomalous ^{8}Be transition sets a rigorous constraint on the mass range of dark matter

Lian-Bao Jia[1,a], **Xue-Qian Li**[2,b]

[1] School of Science, Southwest University of Science and Technology, Mianyang 621010, China
[2] School of Physics, Nankai University, Tianjin 300071, China

Received: 24 August 2016 / Accepted: 7 December 2016 / Published online: 24 December 2016

Abstract The WIMPs are considered to belong to the favorable dark matter (DM) candidates, but the upper bounds on the interactions between DM and standard model (SM) particles obtained by the upgraded facilities of DM direct detection get lower and lower. Researchers turn their attention to the search for less massive DM candidates, i.e. light dark matter of the MeV scale. The recently measured anomalous transition in ^{8}Be suggests that there exists a vectorial boson which may mediate the interaction between DM and SM particles. Based on this scenario, we combine the relevant cosmological data to constrain the mass range of DM, and we have found that there exists a model parameter space where the requirements are satisfied, a range of $10.4 \lesssim m_\phi \lesssim 16.7\,\text{MeV}$ for scalar DM, and $13.6 \lesssim m_V \lesssim 16.7\,\text{MeV}$ for vectorial DM is demanded. Then a possibility of directly detecting such light DM particles via DM–electron scattering is briefly studied in this framework.

1 Introduction

For the time being, we still do not have solid knowledge of dark matter (DM). One of the preferable DM candidates is the weakly interacting massive particle (WIMP), with WIMP masses of the GeV–TeV scale. The recent DM direct detection experiments [1–5] set stringent constraints on the cross section of DM–target nucleus scattering for the GeV–TeV scale DM, and the upper bound of the detection cross section will be reduced to the neutrino limit in the next decade(s). In one respect, of the existence of DM one is convinced by the astronomical observation, while in another respect, the DM particles have not been detected by all the sophisticated experiments. One may ask if our conjecture on the potential mass range of DM is astray, which results in DM evading the present DM direct detections, namely, can the DM particles be much less massive to be in a sub-GeV range, e.g. in MeV (see Refs. [6–13] for some earlier work). In this scenario, the interactions of the light DM particles just render the nucleus to have small recoil energies, which are not observable in available experiments for DM direct detections. In this work, we focus on the MeV scale light DM.

The issue concerning DM refers to two aspects, one is the identities of DM, i.e. what is (are) DM, and another aspect is how DM particles interact among themselves and with SM particles. It is generally believed that the interactions related to the DM sector must be of a new type (new types) beyond the standard model (BSM). In this work, to answer the first question, we do not a priori assume its identity, but let experimental data determine the case; as for the second question, we look for a new BSM interaction which may offer an interpretation for the present observation. The recent ^{8}Be experiment has revealed at 6.8σ an anomalous transition between an excited state ^{8}Be* and the ground state ^{8}Be [14]. The authors of [14,15] argued that this anomaly may be due to unknown nuclear reactions, but a more preferable possibility is that it is caused by emitting a vectorial boson X during $^8\text{Be}^* \to {}^8\text{Be} + X$, which instantly decays into an e^+e^- pair. The new boson X may be the mediator that we look for between DM and SM particle interactions, and this probability is investigated in this paper. A fitted value of X mass is $16.70 \pm 0.35(\text{stat}) \pm 0.5(\text{sys})\,\text{MeV}$ [14], and in this work we adopt the central mass $m_X \simeq 16.7\,\text{MeV}$ in calculations. The interactions of the vector boson X with quarks and leptons via a scheme of BSM has been argued in the literature [15–17]. In this work, the vector boson X discussed in Ref. [15] is of our concern.

For the scattering between possible scalar, vectorial, and fermionic DM and target nucleus, the spin-independent interaction induced by exchanging the vector boson X is dominant (see e.g. Ref. [18]). The vector boson X couples to electron and u, d quarks, and X may also couple to the sec-

[a] e-mail: jialb@mail.nankai.edu.cn
[b] e-mail: lixq@nankai.edu.cn

ond and/or the third generation SM charged leptons and up type/down type quarks with equal couplings to the same type fermions (see e.g. Ref. [16] for more discussion). For the thermal freeze-out DM with such couplings, a DM mass as low as 0.5 GeV has been excluded by the CRESST-II experiment [1]. Thus, the X-mediated sub-GeV DM needs more attention.

Here we focus on the MeV scale DM. The energy released by DM annihilation can modify the cosmic microwave background (CMB), and the recent CMB measurement by the Planck satellite [19] sets a stringent bound on the s-wave annihilation of the MeV scale DM [19,20]. For MeV DM with vector form interaction induced by X, the annihilation of the fermionic DM pair is s-wave dominant, so it is inconsistent with the CMB observation. Thus, the possibility of DM being fermions is disfavored. By contrast, p-wave annihilations of scalar and/or vector DM candidates at freeze-out are tolerable by the CMB result. Thus, we concentrate on the case of scalar and vector DM; the corresponding model parameter space will be derived.

For a DM mass in the range of a few MeV/teens MeV, the big bang nucleosynthesis (BBN) and the effective number of relativistic neutrino $N_{\rm eff}$ at recombination may be altered by the energy release from dark sector annihilations. Thus corresponding observation results will be taken into account to set a lower bound on the DM mass.

As recoils of the target nucleus are small, the scattering between DM and nucleus is not sensitive for DM in MeV region, thus for direct detection for DM one would turn to the DM–electron scattering, which might be employed for the light DM hunting, and the issue was investigated in Refs. [21–23]. In this work the search for DM via its scattering with electron will be discussed for our concerned model.

This work is organized as follows. After this introduction, we present the concrete forms of interactions between SM and DM with new boson X exchanged, and estimate the DM p-wave annihilation rate. Next we take into account the constraints by the BBN and CMB to set the mass range of DM, and numerically evaluate the DM-X coupling for the DM mass range of concern. Then we analyze the detection possibility of the MeV DM via the DM–electron scattering. The last section is devoted to a brief conclusion and discussion.

2 Interactions between SM and DM

Based on the model where the new vector boson X mediates the interaction between the SM particles and scalar/vectorial DM, we will analyze the relevant issues. The couplings of X with SM particles has been discussed in Ref. [15]. The effective X–DM coupling can be set in terms of the DM annihilation cross section at DM thermal freeze-out.

2.1 The couplings

We suppose that X mediates a BSM interaction where the new charge in DM $-$ X interaction is e_D. The SM fermions are of equipped with also a new charge to couple to X, which is parameterized as $e\varepsilon_f$ (in unit of e), and ε_f is relevant to the concerned fermion flavor. Let us first formulate the scattering amplitude between scalar DM and SM particles caused by the new interaction where X stands as the mediator. The new effective interaction is in the form

$$\mathcal{L}_S^i = -e_D X_\mu J^\mu_{\rm DM} + e_D^2 X_\mu X^\mu \phi^* \phi - e\varepsilon_f X_\mu J^\mu_{\rm SM}, \tag{1}$$

where ϕ is the scalar DM field. $J^\mu_{\rm DM}$, $J^\mu_{\rm SM}$ are the currents of scalar DM, SM fermions, respectively, with

$$J^\mu_{\rm DM} = i[\phi^*(\partial^\mu \phi) - (\partial^\mu \phi^*)\phi], \qquad \text{scalar DM}, \tag{2}$$

$$J^\mu_{\rm SM} = \Sigma_f \bar{f}\gamma^\mu f, \qquad \text{SM fermions}. \tag{3}$$

To explain the ^{8}Be anomalous transition, the ε_f of the first generation fermion is derived and its value was presented in Ref. [15] as

$$\varepsilon_u \approx \pm 3.7 \times 10^{-3}, \quad \varepsilon_d \approx \mp 7.4 \times 10^{-3},$$
$$2 \times 10^{-4} \lesssim |\varepsilon_e| \lesssim 1.4 \times 10^{-3}, \quad |\varepsilon_\nu \varepsilon_e| \lesssim 7 \times 10^{-5}. \tag{4}$$

Moreover, if the vector boson X couples to the muon with $|\varepsilon_\mu| \approx |\varepsilon_e|$, the discrepancy between theory and experiment in muon $g-2$ can be moderated [15].

For the vectorial DM field V, the V–X vertices are shown in Fig. 1. The VV^*X vertex is $-ie_D[g^{\mu\nu}(k_2-k_1)^\sigma + g^{\nu\sigma}(k_3-k_2)^\mu + g^{\sigma\mu}(k_1-k_3)^\nu]$, and the VV^*XX vertex is $ie_D^2(g^{\mu\rho}g^{\nu\sigma} + g^{\mu\sigma}g^{\nu\rho} - 2g^{\mu\nu}g^{\rho\sigma})$. The couplings of X in the SM sector are the same as the scalar DM case.

2.2 DM annihilations

For scalar (vectorial) DM, the annihilation $\phi\phi^* \to X \to f\bar{f}$ ($VV^* \to X \to f\bar{f}$) is a p-wave process. When the scalar (vectorial) DM mass m_ϕ (m_V) is above the X boson mass m_X, the annihilation $\phi\phi^* \to XX$ ($VV^* \to XX$) portal is open, as shown in Fig. 2. However, the analyses of Refs. [19,20] indicate that the CMB measurement sets a stringent

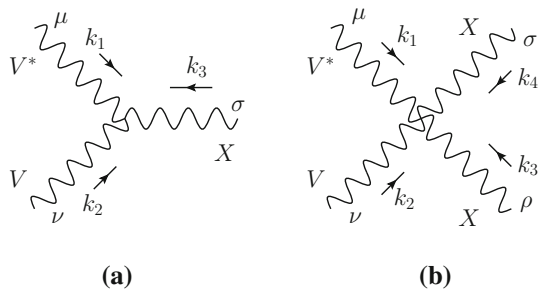

Fig. 1 The vertices of VV^*X, VV^*XX

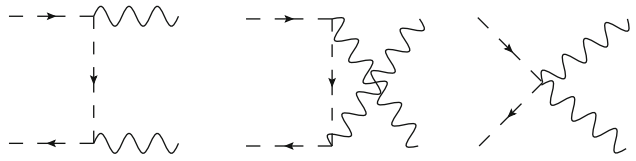

Fig. 2 The annihilation $\phi\phi^* \to XX$. The case of $VV^* \to XX$ is similar

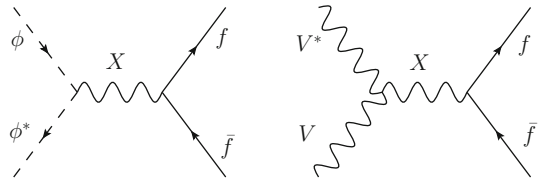

Fig. 3 The annihilations of $\phi\phi^* \to f\bar{f}$ (*left*) and $VV^* \to f\bar{f}$ (*right*)

constraint on the MeV scale DM s-wave annihilation. For DM annihilation channels e^+e^- and $4e$, the upper bounds from CMB on the s-wave annihilations of these two channels are as follows: e.g., for DM with the mass of 5 MeV, the cross sections are about below 2.7×10^{-30}, 4.3×10^{-30} (cm^3/s) for e^+e^-, $4e$, respectively; for DM with the mass of 500 MeV, the cross sections are about below 4.2×10^{-28}, 3.5×10^{-28} (cm^3/s) for e^+e^-, $4e$, respectively. For the MeV scale DM, these constraints are much below the required thermally freeze-out annihilation cross section, and some tunings are needed if the DM s-wave annihilation exists. Thus for thermal freeze-out DM, to avoid the s-wave annihilation in the process $\phi\phi^* \to XX$ ($VV^* \to XX$), the constraint of m_ϕ (m_V) $< m_X$ is mandatory, i.e. the corresponding annihilation is kinematically closed. In addition, as indicated by the ^{8}Be anomaly transition, the X boson predominantly decays into e^+e^-, and this implies that it cannot directly decay into DM, otherwise its decay procedure would be dominated by $X \to \phi\phi^*$ (VV^*). Thus we must demand another constraint m_ϕ (m_V) $> m_X/2$. Therefore, the mass range of DM is $m_X/2 < m_\phi$ (m_V) $< m_X$, and the p-wave annihilation was overwhelming at DM freeze-out.

2.2.1 Scalar DM

Let us first consider the scalar DM. In the mass range $m_X/2 < m_\phi < m_X$, the s-channel annihilation $\phi\phi^* \to X \to f\bar{f}$ is overwhelming at DM freeze-out, as shown in Fig. 3a. In one initial DM particle rest frame, the scalar DM annihilation cross section can be written as

$$\sigma_{\mathrm{ann}} v_r = \frac{1}{2} \frac{e_D^2 e^2 \varepsilon_f^2}{(s-2m_\phi^2)} \frac{\beta_f}{8\pi} \frac{(s-4m_\phi^2)[s-(s-4m_f^2)/3]}{(s-m_X^2)^2 + m_X^2\Gamma_X^2}, \tag{5}$$

where v_r is the relative velocity of the two DM particles. The factor $\frac{1}{2}$ is due to the required $\phi\phi^*$ pair in annihilations, and s is the total invariant squared mass. Γ_X is the decay width of X, and m_f is the mass of the final fermions. The phase space factor β_f is

$$\beta_f = \sqrt{1 - \frac{4m_f^2}{s}}. \tag{6}$$

Parameterizing Eq. (5) in forms of

$$\sigma_{\mathrm{ann}} v_r = a + b v_r^2 + \mathcal{O}(v_r^4), \tag{7}$$

with $s = 4m_\phi^2 + m_\phi^2 v_r^2 + \mathcal{O}(v_r^4)$, we can obtain the result

$$a = 0, \quad b = \frac{e_D^2 e^2 \varepsilon_f^2 \beta_f}{8\pi} \frac{[m_\phi^2 - (m_\phi^2 - m_f^2)/3]}{(4m_\phi^2 - m_X^2)^2 + m_X^2\Gamma_X^2}. \tag{8}$$

With this parameterization, the thermally averaged annihilation cross section at temperature T is [24,25] $\langle \sigma_{\mathrm{ann}} v_r \rangle \approx 6b/x$, with $x = m_\phi/T$. At DM thermal freeze-out temperature T_f, the parameter $x_f = m_\phi/T_f$ is [26,27]

$$x_f \simeq \ln 0.038 c(c+2) \frac{g m_\phi m_{\mathrm{Pl}} 6b/x_f}{\sqrt{g_* x_f}}, \tag{9}$$

where c is a parameter of $O(1)$, and we take $c = 1/2$ for numerical computations. g is the number of degrees of freedom of DM, and $m_{\mathrm{Pl}} = 1.22 \times 10^{19}$ GeV is the Planck mass. g_* is the total number of degrees of freedom as regards the effective relativistic case at the temperature T_f, and we will adopt the data given by Ref. [28]. The relic density of DM is [26,27]

$$\Omega_{\mathrm{DM}} h^2 \simeq \frac{1.07 \times 10^9 x_f}{\sqrt{g_*} m_{\mathrm{Pl}}(\mathrm{GeV})(3b/x_f)}, \tag{10}$$

where h is the Hubble parameter (in units of 100 km/(s·Mpc)).

2.2.2 Vectorial DM

Now consider the vectorial DM. In the mass range $m_X/2 < m_V < m_X$, the annihilation $VV^* \to f\bar{f}$ is overwhelming at DM freeze-out, as shown in Fig. 3b. In the one initial particle rest frame, the vectorial DM annihilation cross section is

$$\sigma_{\mathrm{ann}} v_r = \frac{1}{2} \frac{e_D^2 e^2 \varepsilon_f^2}{(s-2m_V^2)} \frac{\beta_f}{144\pi} \frac{(s-4m_V^2)(s+2m_f^2)}{(s-m_X^2)^2 + m_X^2\Gamma_X^2} \times \left[4 + \frac{7s}{m_V^2} + \frac{s^2}{6m_V^4}\right]. \tag{11}$$

Again parameterizing Eq. (11) in the forms of $\sigma_{\mathrm{ann}} v_r = a + b v_r^2 + \mathcal{O}(v_r^4)$, with $s = 4m_V^2 + m_V^2 v_r^2 + \mathcal{O}(v_r^4)$, we have

$$a = 0, \quad b = \frac{e_D^2 e^2 \varepsilon_f^2}{108\pi} \frac{13\beta_f (2m_V^2 + m_f^2)}{(4m_V^2 - m_X^2)^2 + m_X^2 \Gamma_X^2}. \tag{12}$$

As for the thermally averaged annihilation cross section, the relic density of vectorial DM is similar to the one we derived for scalar DM, replacing the corresponding input parameters.

3 Analysis on X–DM coupling

The energy released from thermal MeV DM annihilation in the early universe can alter the BBN result and the effective number of relativistic neutrinos $N_{\rm eff}$. Even though the effects are not violent, it still can be employed to constrain the lower bound of DM mass. After the DM mass range being set, we will calculate the X–DM coupling by means of the DM thermal freeze-out annihilation cross section.

3.1 DM mass with constraints of $N_{\rm eff}$

In the case of $m_X/2 < m_\phi\ (m_V) < m_X$, the main annihilation product of DM is e^+e^-. DM annihilation might heat the electron–photon plasma before freeze-out in the early universe. If this happens at the time that the neutrino decoupled from the hot bath, the ratio of the neutrino temperature relative to the photon temperature will be lowered, which causes a reduction of the number of the effective neutrino degrees of freedom [12,29]. The abundances of light elements stemming from the primordial nucleosynthesis and the CMB power spectra at the recombination epoch would also be affected. For electron neutrinos, a typical decoupling temperature is $T_d \sim 2.3\,\text{MeV}$ [30]. The value x_f of the thermal freeze-out DM is $x_f \sim 20$. Thus, for the DM of concern, the freeze-out of DM is supposed to be after neutrino decoupling, so the effects of DM annihilation need to be taken into account. For the new boson X, the decay width is

$$\Gamma_X \simeq \frac{e^2 \varepsilon_e^2 (m_X^2 + 2m_e^2)}{12\pi m_X} \sqrt{1 - \frac{4m_e^2}{m_X^2}}. \tag{13}$$

With the mass $m_X \gg T_d$ and X's lifetime much less than 1 second, the contribution from X's entropy to the BBN is negligible.

Here we focus on the constraints from the primordial abundances of light elements ^{4}He and deuterium, denoted by Y_p and y_{DP}, respectively. The abundance values of ^{4}He and deuterium are related to the baryon density $\omega_b \equiv \Omega_b h^2$ and the effective number of relativistic neutrinos $N_{\rm eff}$ (or, in the form of the difference of $\Delta N_{\rm eff} \equiv N_{\rm eff} - 3.046$, where $N_{\rm eff} = 3.046$ is the standard cosmological prediction value [31,32]). The abundances predicted by the BBN are parameterized as $Y_p\ (\omega_b, \Delta N_{\rm eff})$, $y_{DP}\ (\omega_b, \Delta N_{\rm eff})$, and the corresponding Taylor expansion forms can be obtained with the PArthENoPE code [33]. If the value $\omega_b = 0.02226^{+0.00040}_{-0.00039}$ is adopted with the bounds of Planck TT+lowP+BAO [19], the value of $N_{\rm eff}$ is also determined by the constraints of the ^{4}He and deuterium abundances. The range of $N_{\rm eff}$ can be derived with the Planck data, and one has [19]

$$N_{\rm eff} = \begin{cases} 3.14^{+0.44}_{-0.43} & \text{He + Planck TT + lowP + BAO,} \\ 3.01^{+0.38}_{-0.37} & \text{D + Planck TT + lowP + BAO,} \end{cases} \tag{14}$$

where the helium, deuterium abundances given by Aver et al. [34] and Cooke et al. [35] are taken. The updated Planck-only constraint on $N_{\rm eff}$ is [19]

$$N_{\rm eff} = 3.15 \pm 0.23 \quad \text{Planck TT + lowP + BAO.} \tag{15}$$

Considering Eqs. (14) and (15), a lower bound $N_{\rm eff} \gtrsim 2.9$ is taken in the calculations.

In the case that DM mainly couples to the electron–photon plasma and DM particles freeze-out later than the neutrino decoupling, the effective number $N_{\rm eff}$ can be written as [36,37]

$$N_{\rm eff} = 3.046 \left[\frac{I(0)}{I(T_d)}\right]^{\frac{4}{3}}, \tag{16}$$

where $I(T_\gamma)$ is given by

$$\begin{aligned} I(T_\gamma) &= \frac{1}{T_\gamma^4}(\rho_{e^+e^-} + \rho_\gamma + \rho_{\rm DM} + p_{e^+e^-} + p_\gamma + p_{\rm DM}) \\ &= \frac{11}{45}\pi^2 + \frac{g}{2\pi^2}\int_{y=0}^{\infty} {\rm d}y \frac{y^2}{e^\xi \pm 1}\left(\xi + \frac{y^2}{3\xi}\right) \end{aligned} \tag{17}$$

and

$$\xi = \sqrt{y^2 + (m_{\rm DM}/T_\gamma)^2}. \tag{18}$$

Here T_γ is the photon temperature, and the integration variable is $y = p_{\rm DM}/T_\gamma$. The plus/minus sign is for fermionic/bosonic DM particles, respectively. For the bosonic DM of concern, the parameter values of the degrees of freedom are $g_B = 2$, $g_B = 6$, and the masses $m_{\rm DM} = m_\phi, m_V$ are corresponding to the scalar and vectorial DM, respectively. The effective number $N_{\rm eff}$ as a function of $m_{\rm DM}/T_d$ is shown in Fig. 4. Taking the lower bound $N_{\rm eff} \gtrsim 2.9$, we can obtain $m_{\rm DM}/T_d \gtrsim 5.2, 6.8$ for scalar and vectorial DM, respectively. As the neutrino decoupling is not a sudden process (for more details, see e.g. Refs. [30–32,38]), here we take $T_d \gtrsim 2$ MeV as a lower bound. Thus, the mass range of DM is derived,

$$\begin{cases} 10.4 \lesssim m_\phi \lesssim 16.7 \ \text{(MeV)} & \text{scalar DM,} \\ 13.6 \lesssim m_V \lesssim 16.7 \ \text{(MeV)} & \text{vectorial DM.} \end{cases} \tag{19}$$

3.2 Numerical result for the X–DM coupling

As the DM mass range being set, we turn to an investigation of the X–DM coupling. The DM relic density is 0.1197 ± 0.0042 [19]. According to the DM thermally averaged annihilation

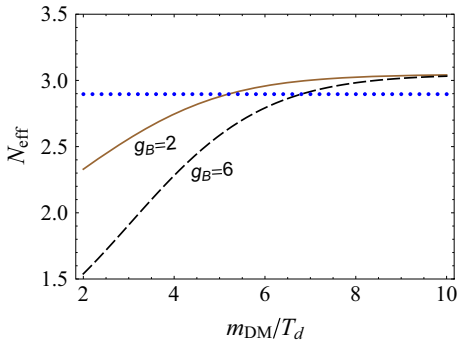

Fig. 4 The effective number $N_{\rm eff}$ as a function of $m_{\rm DM}/T_d$. The *solid*, *dashed curves* are the scalar and vectorial DM of concern, respectively. The *dotted curve* is for the *lower* bound $N_{\rm eff} = 2.9$

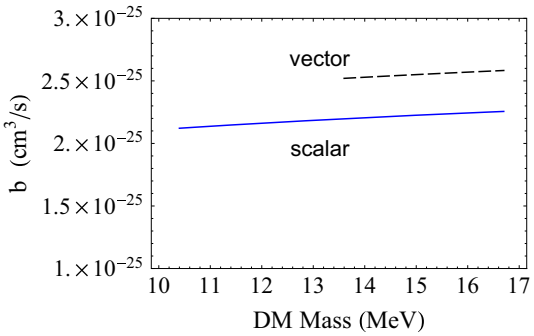

Fig. 5 The parameter b as a function of the DM mass. The *solid*, *dashed curves* are the scalar and vectorial DM of concern, respectively

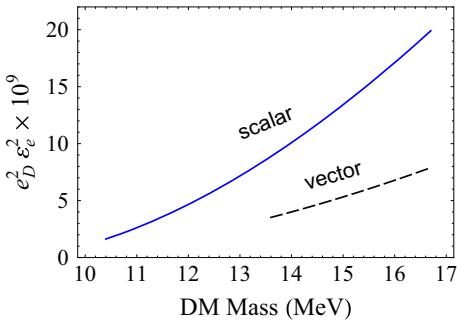

Fig. 6 The values of $e_D^2\varepsilon_e^2$ as a function of the DM mass. The solid, dashed curves are the scalar, vectorial DM, respectively

cross section $\langle\sigma_{\rm ann}v_r\rangle \approx 6b/x_f$ at T_f, the numerical results of b are shown in Fig. 5, with the solid, dashed curves corresponding to the scalar and vectorial DM, respectively. After the values of b defined in Eq. (7) are obtained, the X–DM coupling couplings are also determined. The numerical results of $e_D^2\varepsilon_e^2$ are depicted in Fig. 6. Considering the value of ε_e given by Eq. (4), we can obtain $e_D^2/4\pi < 1$, and thus the X–DM coupling is sufficiently small so that the perturbation may apply.

4 DM–electron scattering

Now let us turn to an investigation of the possibility of detecting the light DM of the MeV scale by the earth detector.

For the light DM particles, since the recoil of the target nucleus is too small to be clearly observed, one may not detect the arrival of DM via the scattering between the MeV DM and target nucleus. Instead, the DM–electron scattering can be employed for the MeV DM hunting. The DM–electron scattering has been investigated in Refs. [21–23]. The target atomic electron is in a bound state, and the typical momentum transfer q is of the order αm_e of a few eV, which may cause excitation/ionization of the electron in inelastic scattering processes. In this work, we study the signals of individual electrons induced by DM–electron scattering. Here, we take the form of the DM–electron scattering cross section as given by Ref. [39], and for scalar DM, that is,

$$\begin{aligned}\bar{\sigma}_e &= \frac{\mu_{\phi e}^2}{16\pi m_\phi^2 m_e^2}\overline{|\mathcal{M}_{\phi e}(q)|^2}\big|_{q^2=\alpha^2 m_e^2} \times |F_{\rm DM}(q)|^2 \\ &\simeq \frac{4\alpha e_D^2\varepsilon_e^2\mu_{\phi e}^2}{m_X^4},\end{aligned} \tag{20}$$

with $\mu_{\phi e}$ being the ϕ–electron reduced mass, and $F_{\rm DM}(q) \simeq 1$ for $m_X \gg \alpha m_e$.

For vectorial DM, the DM–electron scattering cross section is

$$\begin{aligned}\bar{\sigma}_e &= \frac{\mu_{Ve}^2}{16\pi m_V^2 m_e^2}\overline{|\mathcal{M}_{Ve}(q)|^2}\big|_{q^2=\alpha^2 m_e^2} \times |F_{\rm DM}(q)|^2 \\ &\simeq \frac{4\alpha e_D^2\varepsilon_e^2\mu_{Ve}^2}{m_X^4},\end{aligned} \tag{21}$$

with μ_{Ve} being the V–electron reduced mass.

As the value of $e_D^2\varepsilon_e^2$ is fixed, the DM–electron scattering cross section $\bar{\sigma}_e$ can be obtained. The numerical result of $\bar{\sigma}_e$ is shown in Fig. 7, where it is noted that the scattering cross section is independent of the momentum transfer ($F_{\rm DM}(q) = 1$). The upper solid, upper dashed curves are for the scalar, vectorial DM, respectively, and the dot-dashed curve is the excluded bound set by the XENON10 data [40]. It can be seen that, considering the constraint of XENON10, there exist parameter spaces for the scalar and vectorial DM to satisfy the constraints.

Now we give a brief discussion as regards the background in the DM–electron scattering. One irreducible background is from neutrino–electron scattering, which sets the ultimate limit to the sub-GeV DM direct detections. Fortunately, the DM annual modulation effect from the motion of the earth can be employed to reduce the neutrino background [39,41,42]. The teens MeV DM of concern could be probed via the inelastic processes of DM–electron scatterings, e.g. the individual electron signals by the future noble gas and

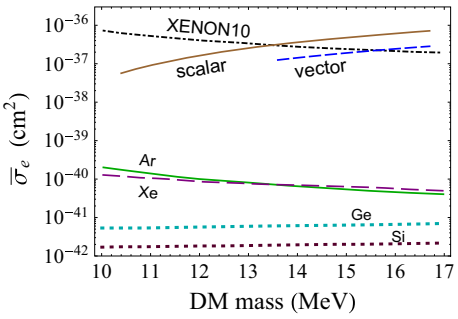

Fig. 7 The DM–electron scattering cross section $\bar{\sigma}_e$ as a function of the DM mass with the parameter $F_{\rm DM}(q) = 1$. The upper solid, upper dashed curves are the scalar and vectorial DM, respectively. The dot-dashed curve is the excluded bound set by the XENON10 data [40]. The lower solid, lower dashed curves are the 95% confidence level exclusion reach of single electron detections set by the 1 kg·year exposure of Ar, Xe [39], respectively. The upper, lower square curves are the 95% confidence level exclusion reach of single electron detections set by the 1 kg·year exposure of Ge, Si [43], respectively

semiconductor targets. For Ar, Xe [39] and Ge, Si [43] with 1 kg·year exposure, the exclusion reach at 95% confidence level via single electron detection is also shown in Fig. 7. Further explorations of DM–electron scatterings are needed, both in theory and experiment.

5 Conclusion and discussion

The MeV scalar and vectorial DM has been studied in this work, with the new boson X indicated by the ^{8}Be anomalous transition being the mediator. Considering the constraints of the DM direct detection and CMB observation, we find that, for the case of $m_X/2 < m_\phi\ (m_V) < m_X$, the p-wave dominant annihilation of DM at freeze-out does not conflict with the observed data so far. The primordial abundances of light elements and the effective number of relativistic neutrinos $N_{\rm eff}$ at recombination are sensitive to the DM with a mass of a few MeV to teens MeV; thus the corresponding observed results have been employed to set a lower bound on the DM mass. Taking the combined lower bounds $N_{\rm eff} \gtrsim 2.9$ and the neutrino decoupling temperature $T_d \gtrsim 2\,$MeV, we derive a mass range of DM: $10.4 \lesssim m_\phi \lesssim 16.7\,$MeV for scalar DM, and $13.6 \lesssim m_V \lesssim 16.7\,$MeV for vectorial DM.

For the teens MeV scalar and vectorial DM of concern, the numerical result of the DM–X coupling is derived in terms of the DM thermally averaged annihilation cross section. Once this coupling is set, the strength of the interaction between DM and SM particles is determined.

The DM–electron scattering is employed for the teens MeV DM hunting. We investigate the signal of the individual electrons in DM–electron scattering, and the scattering cross section $\bar{\sigma}_e$ is calculated for the DM mass range of concern. We find that, considering the constraint of XENON10, there are still parameter spaces left for the teens MeV scalar and vectorial DM to be observed. Beside the individual electrons, signals of individual photons, individual ions, and heat/phonons can also be employed to explore the MeV DM–electron scattering (see e.g. Ref. [39,44] for more), even though the ion signal is probably too weak for detection. The teens MeV DM of concern could be probed by the future noble gas and semiconductor targets via the DM–electron scattering. In fact, the wave function of electron in the bound state for a certain target material needs to be considered to guarantee the prediction power. It is noted that the detection possibilities and efficiency of DM are target dependent.

As discussed in Ref. [45], the new boson X may be detectable at the e^+e^- collider, such as BESIII and BaBar. The new boson X may also give an interpretation about the NuTeV anomaly [46]. For the teens MeV scalar and vectorial DM of concern, further investigations both in theory and experiment aspects are needed. We look forward to the exploration of the X-portal DM in the future.

Acknowledgements This work was partially supported by the National Natural Science Foundation of China under Contract Nos. 11505144, 11375128 and 11135009, and the Research Fund for the Doctoral Program of the Southwest University of Science and Technology under Contract No. 15zx7102.

References

1. G. Angloher et al. [CRESST Collaboration], Eur. Phys. J. C **76**(1), 25 (2016). arXiv:1509.01515 [astro-ph.CO]
2. R. Agnese et al. [SuperCDMS Collaboration], Phys. Rev. Lett. **116**(7), 071301 (2016). arXiv:1509.02448 [astro-ph.CO]
3. D.S. Akerib et al. [LUX Collaboration], Phys. Rev. Lett. **116**(16), 161301 (2016). arXiv:1512.03506 [astro-ph.CO]
4. E. Aprile et al. [XENON Collaboration], JCAP **1604**(04), 027 (2016). arXiv:1512.07501 [physics.ins-det]
5. A. Tan et al. [PandaX-II Collaboration], Phys. Rev. Lett. **117**(12), 121303 (2016). arXiv:1607.07400 [hep-ex]
6. P. Fayet, Nucl. Phys. B **187**, 184 (1981)
7. C. Boehm, T.A. Ensslin, J. Silk, J. Phys. G **30**, 279 (2004). arXiv:astro-ph/0208458
8. C. Boehm, D. Hooper, J. Silk, M. Casse, J. Paul, Phys. Rev. Lett. **92**, 101301 (2004). arXiv:astro-ph/0309686
9. D. Hooper, F. Ferrer, C. Boehm, J. Silk, J. Paul, N.W. Evans, M. Casse, Phys. Rev. Lett. **93**, 161302 (2004). arXiv:astro-ph/0311150
10. C. Boehm, P. Fayet, Nucl. Phys. B **683**, 219 (2004). arXiv:hep-ph/0305261
11. P. Fayet, Phys. Rev. D **70**, 023514 (2004). arXiv:hep-ph/0403226
12. P.D. Serpico, G.G. Raffelt, Phys. Rev. D **70**, 043526 (2004). arXiv:astro-ph/0403417
13. P. Fayet, Phys. Rev. D **74**, 054034 (2006). arXiv:hep-ph/0607318

14. A.J. Krasznahorkay et al., Phys. Rev. Lett. **116**(4), 042501 (2016). arXiv:1504.01527 [nucl-ex]
15. J.L. Feng, B. Fornal, I. Galon, S. Gardner, J. Smolinsky, T.M.P. Tait, P. Tanedo, Phys. Rev. Lett. **117**(7), 071803 (2016). arXiv:1604.07411 [hep-ph]
16. P.H. Gu, X.G. He, arXiv:1606.05171 [hep-ph]
17. J.L. Feng, B. Fornal, I. Galon, S. Gardner, J. Smolinsky, T.M.P. Tait, P. Tanedo, arXiv:1608.03591 [hep-ph]
18. M. Freytsis, Z. Ligeti, Phys. Rev. D **83**, 115009 (2011). arXiv:1012.5317 [hep-ph]
19. P.A.R. Ade et al. [Planck Collaboration], arXiv:1502.01589 [astro-ph.CO]
20. T.R. Slatyer, Phys. Rev. D **93**(2), 023527 (2016). arXiv:1506.03811 [hep-ph]
21. R. Bernabei et al., Phys. Rev. D **77**, 023506 (2008). arXiv:0712.0562 [astro-ph]
22. A. Dedes, I. Giomataris, K. Suxho, J.D. Vergados, Nucl. Phys. B **826**, 148 (2010). arXiv:0907.0758 [hep-ph]
23. J. Kopp, V. Niro, T. Schwetz, J. Zupan, Phys. Rev. D **80**, 083502 (2009). arXiv:0907.3159 [hep-ph]
24. M. Srednicki, R. Watkins, K.A. Olive, Nucl. Phys. B **310**, 693 (1988)
25. P. Gondolo, G. Gelmini, Nucl. Phys. B **360**, 145 (1991)
26. E.W. Kolb, M.S. Turner, Front. Phys. **69**, 1 (1990)
27. K. Griest, D. Seckel, Phys. Rev. D **43**, 3191 (1991)
28. M. Drees, F. Hajkarim, E.R. Schmitz, JCAP **1506**(06), 025 (2015). arXiv:1503.03513 [hep-ph]
29. E.W. Kolb, M.S. Turner, T.P. Walker, Phys. Rev. D **34**, 2197 (1986)
30. K. Enqvist, K. Kainulainen, V. Semikoz, Nucl. Phys. B **374**, 392 (1992)
31. A.D. Dolgov, Phys. Rept. **370**, 333 (2002). arXiv:hep-ph/0202122
32. G. Mangano, G. Miele, S. Pastor, T. Pinto, O. Pisanti, P.D. Serpico, Nucl. Phys. B **729**, 221 (2005). arXiv:hep-ph/0506164
33. O. Pisanti, A. Cirillo, S. Esposito, F. Iocco, G. Mangano, G. Miele, P.D. Serpico, Comput. Phys. Commun. **178**, 956 (2008). arXiv:0705.0290 [astro-ph]
34. E. Aver, K.A. Olive, R.L. Porter, E.D. Skillman, JCAP **1311**, 017 (2013). arXiv:1309.0047 [astro-ph.CO]
35. R. Cooke, M. Pettini, R.A. Jorgenson, M.T. Murphy, C.C. Steidel, Astrophys. J. **781**(1), 31 (2014). arXiv:1308.3240 [astro-ph.CO]
36. C.M. Ho, R.J. Scherrer, Phys. Rev. D **87**(2), 023505 (2013). arXiv:1208.4347 [astro-ph.CO]
37. C.M. Ho, R.J. Scherrer, Phys. Rev. D **876**, 065016 (2013). arXiv:1212.1689 [hep-ph]
38. S. Hannestad, Phys. Rev. D **65**, 083006 (2002). arXiv:astro-ph/0111423
39. R. Essig, J. Mardon, T. Volansky, Phys. Rev. D **85**, 076007 (2012). arXiv:1108.5383 [hep-ph]
40. R. Essig, A. Manalaysay, J. Mardon, P. Sorensen, T. Volansky, Phys. Rev. Lett. **109**, 021301 (2012). arXiv:1206.2644 [astro-ph.CO]
41. S.K. Lee, M. Lisanti, S. Mishra-Sharma, B.R. Safdi, Phys. Rev. D **92**(8), 083517 (2015). arXiv:1508.07361 [hep-ph]
42. A.K. Drukier, K. Freese, D.N. Spergel, Phys. Rev. D **33**, 3495 (1986)
43. R. Essig, M. Fernandez-Serra, J. Mardon, A. Soto, T. Volansky, T.T. Yu, JHEP **1605**, 046 (2016). arXiv:1509.01598 [hep-ph]
44. S. Derenzo, R. Essig, A. Massari, A. Soto, T.T. Yu, arXiv:1607.01009 [hep-ph]
45. L.B. Chen, Y. Liang, C.F. Qiao, arXiv:1607.03970 [hep-ph]
46. Y. Liang, L.B. Chen, C.F. Qiao, arXiv:1607.08309 [hep-ph]